CrystEngComm

Accepted Manuscript

ROYAL SOCIETY OF CHEMISTRY

www.rsc.org/crystengcomm

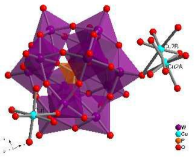

$Cu_{1.5}(H_2O)_{7.5}PW_{12}O_{40}.4.75(H_2O)$

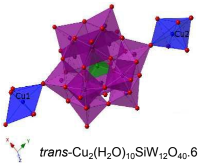

trans-$Cu_2(H_2O)_{10}SiW_{12}O_{40}.6(H_2O)$

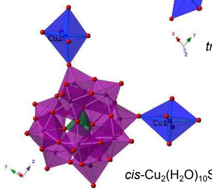

cis-$Cu_2(H_2O)_{10}SiW_{12}O_{40}.6(H_2O)$

Journal Name

ARTICLE

Disorder and Polymorphism in Cu(II)-polyoxometalate complexes: $[Cu_{1.5}(H_2O)_{7.5}PW_{12}O_{40}]\cdot4.75H_2O$, *cis*- & *trans*-$[Cu_2(H_2O)_{10}SiW_{12}O_{40}]\cdot6H_2O$

Received 00th January 20xx,
Accepted 00th January 20xx

DOI: 10.1039/x0xx00000x

www.rsc.org/

Sneha R. Bajpe[a,*], Sebastian Henke[b], Jung-Hoon Lee[a], Paul D. Bristowe[a] and Anthony K. Cheetham[a,*]

Three highly crystalline Cu(II)-polyoxometalate (POM) complexes, $[Cu_{1.5}(H_2O)_{7.5}PW_{12}O_{40}]\cdot4.75H_2O$ and *cis*- and *trans*-$[Cu_2(H_2O)_{10}SiW_{12}O_{40}]\cdot6H_2O$, were successfully synthesized and characterized by single crystal and powder X-ray diffraction as well as thermogravimetric analysis. All complexes feature octahedrally coordinated, Jahn-Teller-distorted Cu^{II} centres, which are coordinated by one terminal oxygen atom of the POM anion and five water molecules. The crystal structure of $[Cu_{1.5}(H_2O)_{7.5}PW_{12}O_{40}]\cdot4.75H_2O$, reveals four-fold disorder at one of the two Cu-sites, whereas $[Cu_2(H_2O)_{10}SiW_{12}O_{40}]\cdot6H_2O$ crystallizes in two fully-ordered polymorphic forms: a monoclinic structure containing an angled *cis* configuration of the Cu-POM-Cu molecule and a triclinic structure containing a linear *trans* configuration. Density functional theory (DFT) calculations show that the *cis* polymorph of $[Cu_2(H_2O)_{10}SiW_{12}O_{40}]\cdot6H_2O$ is more stable than the *trans* form by about 30 kJ/mol.

Introduction

Since their discovery, polyoxometalates (POMs) have attracted enormous attention in inorganic chemistry. POMs are transition metal clusters with discrete metal-oxygen bonds around a central ion.[1,2] They have well-defined topologies with intriguing physical and chemical properties and an astounding range of redox transformations.[1-12] Easy synthesis and large structural variation, coupled with diverse applications in industry,[2,4] has led to their immense popularity. Structural diversity in POMs can be achieved by combining them with many elements of the periodic table, and many of the clusters containing transition-metals have interesting magnetic,[13] optical,[14] catalytic,[1] or electronic properties.[15]

Among the several different families of POMs, polyoxo-tungstates, -molybdates and -vanadates are the most widely studied[16-19] due to their varied applications in industry as homogeneous[16,20-22] and heterogeneous catalysts.[1,23] Although these POMs have great potential in the catalysis industry,[1,24] Keggin-type tungstophosphoric acid $[H_3PW_{12}O_{40}\cdot xH_2O]$ and tungstosilicic acid $[H_4SiW_{12}O_{40}\cdot xH_2O]$ exhibit poor yields in some acid-catalysed reactions such as isopropanol dehydration.[25] However, salts of these POMs can show significant improvements in catalytic activity for the same reactions.[26,27]

A huge variety of salts of these polyoxometalates have therefore been synthesized by simultaneous reaction of the acid with almost all of the transition metals.[19,22] Among the various transition metals tested, Cu^{II} has so far outnumbered its counterparts by exhibiting higher flexibility due to its different coordinating ability (square planar, square pyramidal, trigonal-bipyramidal and octahedral).[16,17] In addition to this, Jahn-Teller and pseudo-Jahn-Teller effects of the Cu^{II} octahedral and square pyramidal geometries make Cu^{II} extremely versatile in its structural adaptability, forming several interesting configurations.[16] For example, Cu^{II} forms a giant wheel-shaped Cu_{20}-POM[28] and dimeric clusters[9,24] when reacted with different polyoxoanions.

The synthesis of several Cu^{II}-polyoxometalate complexes[29-34] has rendered POMs as potential candidates for a number of catalytic applications, thus eliminating the troubles associated with naked POMs under reaction conditions. In this regard, Méndez et. al.[35] have reported the use of Al^{III} and Cu^{II} salts of POMs resulting in higher catalytic yields in acylation reactions.

a, Dr. Sneha R. Bajpe, Prof. Anthony K. Cheetham*
Email: sb974@cam.ac.uk, akc30@cam.ac.uk

a Department of Materials Science and Metallurgy,
University of Cambridge,
27 Charles Babbage Road, Cambridge CB3 0FS, United Kingdom.

b Lehrstuhl für Anorganische Chemie II, Ruhr-Universität Bochum
44780 Bochum, Germany.

Electronic Supplementary Information (ESI) available: ESI contains crystallographic information obtained form single crystal X-ray diffraction, IR, TGA and PXRD data.
CCDC: Compound **1**- 1420704, Compound ***2c*** at 123 K - 1466493, Compound ***2c*** at 293 K - 1420705 , Compound ***2t*** - 1420706.

Following this, Yadav et. al.[26] and Purnima et. al.[27] reported enhanced catalytic activity of Cu^{II} salts of tunstophosphoric acid in different acid catalysed reactions. Although they have successfully obtained the Cu^{II}-POM salts in powder form, the crystal structure could not be established due to very poor crystallinity. Méndez et. al.[35] have specifically pointed out the need to establish the crystal structures of the Cu-POM compounds.

We have been interested in Cu-based POM architectures for several years and have studied the templating behaviour[36,37] of POMs in the formation of Cu-based organic-inorganic hybrids. For example, in the presence of Keggin POMs, Cu^{II} undergoes dimerization and forms an HKUST-1 type hybrid framework with the organic linker 1,3,5-benzene-tricarboxylate (BTC).[37] This work led to the study of POM-templated metal-organic frameworks for applications in luminescence[38,39] and catalysis.[40] Although the formation of copper paddlewheel dimers in the presence of Keggin POMs was definitively established, the question whether copper alone can stabilize the formation of a Cu-POM complex by behaving as a counter-cation remained unresolved. In the present work, we report the successful synthesis and crystallographic structural characterisation of pure Cu^{II} salts of tungstophosphoric acid, $[Cu_{1.5}(H_2O)_{7.5}PW_{12}O_{40}]\cdot 4.75H_2O$, and tungstosilicic acid, $[Cu_2(H_2O)_{10}SiW_{12}O_{40}]\cdot 6H_2O$, in the absence of any alkali metal (such as Na^+, K^+, etc) acting as an additional counter cation. Interestingly, we also found that $[Cu_2(H_2O)_{10}SiW_{12}O_{40}]\cdot 6H_2O$ can exist in two polymorphic forms displaying either a *cis* or a *trans* configuration of the decorated POM. We present a detailed structural analysis of different Cu^{II}-polyoxometalate complexes in addition to the results of first-principle density functional theory (DFT) calculations, which enable us to compare the stabilities of the *cis*- and *trans*-polymorphs. On the basis of the DFT calculations, we propose that water molecules play a key role in stabilizing the crystal structures *via* hydrogen bonding.

Results and Discussion

We have explored the formation of Cu^{II} salts of two different polyoxoanions - $[PW_{12}O_{40}]^{3-}$ and $[SiW_{12}O_{40}]^{4-}$ - by simple room temperature crystallisation of the respective copper salts from the protonated acids and copper nitrate in an ethanol:H_2O mixture. The resulting copper salts of these POMs, with the structural formulae $[Cu_{1.5}(H_2O)_{7.5}PW_{12}O_{40}]\cdot 4.75H_2O$ and $[Cu_2(H_2O)_{10}SiW_{12}O_{40}]\cdot 6H_2O$, respectively, were characterized by single crystal, powder X-ray diffraction, ^{31}P NMR, IR and thermogravimetric analysis (TGA). Both $[Cu_{1.5}(H_2O)_{7.5}PW_{12}O_{40}]\cdot 4.75H_2O$ and $[Cu_2(H_2O)_{10}SiW_{12}O_{40}]\cdot 6H_2O$ resulted in the formation of large transparent-blue single crystals.

Structure of compound 1: $[Cu_{1.5}(H_2O)_{7.5}PW_{12}O_{40}]\cdot 4.75H_2O$

Crystallographic details are given in Table 1 and supplementary information tables S1 & S2. The structure of the Cu^{II} salt of phosphotungstate contains discrete polyoxoanion $[PW_{12}O_{40}]^{3-}$ units with 1.5 Cu^{II} ions coordinated to these clusters; these behave as charge balancing cations since exactly 1.5 Cu^{II} ions are needed to balance the negative charge of each $[PW_{12}O_{40}]^{3-}$. The $[PW_{12}O_{40}]^{3-}$ cluster is connected to a $Cu(H_2O)_5$ unit, with the sixth coordinating site of the copper provided by one of the terminal oxygen atoms of the $[PW_{12}O_{40}]^{3-}$ cluster; this is Cu1 in Figure 1. There is then an additional $Cu(H_2O)_5$ unit (Cu2), which is only half occupied for charge balance (hence the 1.5 Cu^{II} per $[PW_{12}O_{40}]^{3-}$ unit in total). In the asymmetric unit, this half occupied $Cu(H_2O)_5$ cation is disordered over two positions, such that, each of the two positions has 25% occupancy. Due to the severe disorder of this $Cu(H_2O)_5$ unit, structure refinement could only be performed by restraining the Cu-O distances for equatorial O atoms to 1.98±0.02 Å and to 2.36±0.02 Å for the axial O atoms for both crystallographically distinct fragments (Cu2A and Cu2B ions; see cif and supplementary information tables S1 & S2 for further details). The disordered $Cu(H_2O)_5$ unit is shared equally by two adjacent $[PW_{12}O_{40}]^{3-}$ clusters, leading to fourfold disorder overall. The structure contains 12.25 molecules of H_2O per asymmetric unit, which was confirmed by thermogravimetric analysis (TGA) (supplementary information Figure S6(a) and table S9). Of these water molecules, 7.5 are coordinated to copper and the balance of 4.75 molecules per formula unit lie between the POM clusters.

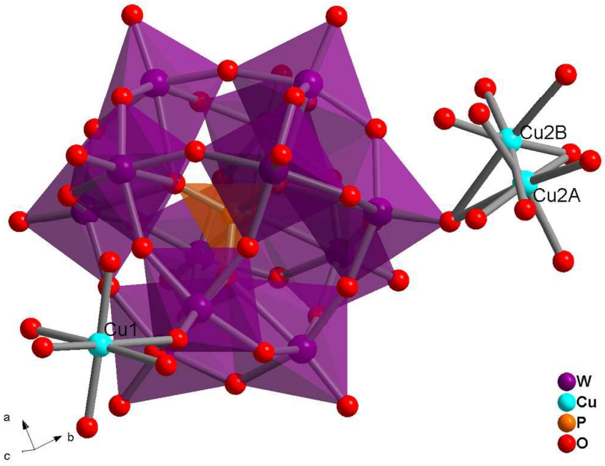

Figure 1. Compound 1: $[Cu_{1.5}(H_2O)_{7.5}PW_{12}O_{40}]\cdot 4.75H_2O$ exhibiting disorder at one of the Cu^{II} centers. Cu2 is fourfold disordered (only the two crystallographically independent fragments are shown here) with Cu2A and Cu2B possessing 25% occupancy each. The uncoordinated water molecules are removed from the image for visual clarity.

Structures of compounds 2*c* & 2*t*: monoclinic and triclinic $[Cu_2(H_2O)_{10}SiW_{12}O_{40}]\cdot 6H_2O$

In order to investigate the behaviour of Cu^{II} with a second Keggin cluster, we explored its reaction with the analogous $[SiW_{12}O_{40}]^{4-}$ polyoxoanion. Keggin-tungstosilicates $[SiW_{12}O_{40}]^{4-}$ are generally more stable than other tungsten heteropolyanions,[41] and since $[SiW_{12}O_{40}]^{4-}$ requires 4+ charge for charge balance, we postulated that two Cu^{II} ions would be able to coordinate to a single $[SiW_{12}O_{40}]^{4-}$ anion and do not exhibit disorder as in compound **1**. A different set of reactions were performed with the $[SiW_{12}O_{40}]^{4-}$ Keggins and Cu^{II}, maintaining the synthesis conditions similar to that of the $[PW_{12}O_{40}]^{3-}$ Keggin. As predicted, we were able to form highly crystalline, transparent-blue crystals of $[Cu_2(H_2O)_{10}SiW_{12}O_{40}]\cdot 6H_2O$. Surprisingly, we realized that the $[Cu_2(H_2O)_{10}SiW_{12}O_{40}]\cdot 6H_2O$ was not phase pure and further investigation revealed that it was a mixture of monoclinic and triclinic polymorphs with the same $[Cu_2(H_2O)_{10}SiW_{12}O_{40}]\cdot 6H_2O$ composition. The monoclinic isomer exhibits a *cis* configuration of the $Cu(H_2O)_5$–POM–$Cu(H_2O)_5$ cluster while the triclinic one features the related *trans* configuration. Although Mo and V based mixed-polyoxoanions exhibit isomerism[5] within the POM itself, we believe that this is the first time that *cis* and *trans* isomerism has been observed in decorated polyoxoanions.

Crystallographic details for **2*c*** and **2*t*** measured at 123 K are given in Table 1 and supplementary information tables S5-S8. The two Cu^{II} compounds of tungstosilicic acid contain discrete polyoxometalate clusters of $[SiW_{12}O_{40}]^{4-}$ with two Cu^{II} cations balancing the negative charge. In both cases, the Keggin cluster, $[SiW_{12}O_{40}]^{4-}$, coordinates via two terminal oxygen atoms to the two crystallographically distinct $Cu(H_2O)_5$ units, and these two $Cu(H_2O)_5$ units are located at different positions(*cis* and *trans*) in the two polymorphs(Figure 2 and 3 respectively. Both crystal forms contain $16H_2O$ molecules per formula unit, 10 attached to the copper ions and 6 lying between the POM clusters. This was confirmed by TGA (supplementary information-Figure S6(b) & table S9). Figures 2 and 3 appear to indicate that these water molecules are responsible for stabilizing the crystal structure *via* various types of hydrogen-bonding. Note, to, that compound **2*c*** is isostructural with compound **1** (see Table 1), indicating that the $Cu(H_2O)_5$ units adopt a *cis* configuration in the phosphotungstate compound.

At room temperature the bulk of the polycrystalline product of compound **2** was largely dominated by the monoclinic phase, as confirmed by a Rietveld refinement of PXRD data (supplementary information-Figure S7, S9 & table S10). The single crystal diffraction data for all compounds discussed here have been recorded at similarly low temperatures (approx. 123 – 125 K). This suggests that the two polymorphs of compound **2** are not simply interconverting as a function of temperature. Rather **2*t*** seems to be a kinetic intermediate, which is thermodynamically less stable than the main phase **2*c*** (see below). The crystallographic details of the measurement performed at 293 K are given in detail in the supplementary information (table S3 & S4, CCDC No. 1420705). Crystallographic details for **2*c*** and **2*t*** measured at 123 K are given in Table 1 and supplementary information tables S5-S8.

Table 1: Crystal data for compound **1** and compound **2*c*** & **2*t***.

Empirical formula	$H_{24.5}Cu_{1.5}O_{52.25}PW_{12}$ Compound 1		$H_{32}Cu_2O_{56}SiW_{12}$ Compound 2*c*		$H_{32}Cu_2O_{56}SiW_{12}$ Compound 2*t*	
CCDC	1420704		1466493		1420706	
Formula weight	3193.17		3289.62		3289.62	
Crystal system	Monoclinic ($P2_1/n$)		Monoclinic ($P2_1/n$)		Triclinic (P-1)	
			Experiment	**DFT**	**Experiment**	**DFT**
a, Å	12.9417(2)		12.9010(3)	12.806	12.8897(4)	12.876
b, Å	21.8435(3)		22.1952(4)	22.038	14.0070(5)	14.015
c, Å	15.0559(2)		15.3468(3)	15.294	15.3382(4)	15.222
α, deg	90		90	90	63.169(3)	62.62
β, deg	94.1800(13)		94.432(2)	94.14	71.079(3)	70.09
γ, deg	90		90	90	63.827(3)	63.42
V, $Å^3$	4244.85(11)		4381.25(16)	4304.69	2190.49(15)	2149.66
Z	4		4		2	
ρ_{calcd}, g cm^{-3}	4.997		4.987		4.988	
μ, cm^{-1}	33.273		32.476		32.478	
T, K	123(1)		123.7(6)		125(2)	
F(000)	5556.0		5760.0		2880.0	
Final *R* indexes [$I \geq 2\sigma(I)$]	R_1= 0.0291	wR_2= 0.0635	R_1= 0.0353	wR_2= 0.0553	R_1= 0.0266	wR_2= 0.0576
Final *R* indexes [all data]	R_1= 0.0360	wR_2= 0.0656	R_1= 0.0276	wR_2= 0.0575	R_1 =0.0310	wR_2= 0.0590

One of the prominent features of compounds **2*c*** and **2*t*** is that the water molecules play a key role in stabilizing the crystal structures *via* hydrogen-bonding. Unfortunately, the H atoms of the water molecules could not be located based on the single crystal X-ray diffraction data due to weak scattering contrast. According to our energy-minimised DFT calculations which have enabled us to include precise coordinates for the hydrogen atoms on the water molecules, there are four different types of hydrogen-bonds as shown in Figure. 2(b): hydrogen-bonding between (i) Keggin W-O groups and water molecules connected to Cu ($W\text{-}O\cdots H_2O\text{-}Cu$), (ii) water molecules connected to Cu and water molecules between the Keggins ($Cu\text{-}H_2O\cdots H_2O$), (iii) water molecule between the Keggins and O atoms on W ($H_2O\cdots O\text{-}W$), and (iv) H atoms on two water molecules ($H_2O\cdots H_2O$). In fact, these hydrogen-bonds provide links between the clusters and thereby stabilize the whole structure.

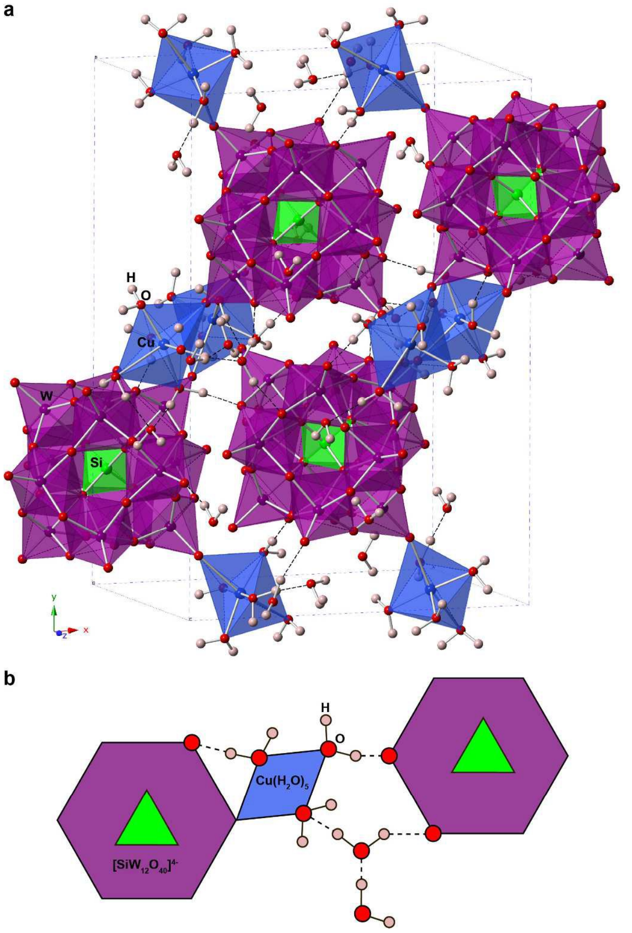

Figure 2: Compound 2*c*: (a) Image showing the monoclinic $[Cu_2(H_2O)_{10}SiW_{12}O_{40}]\cdot 6H_2O$ structure after the addition of H atoms followed by DFT optimization/MD simulations. (b) Schematic view of various types of hydrogen-bonds between two $[SiW_{12}O_{40}]^{4-}$ units. The dotted lines indicate hydrogen-bonds between oxygen and hydrogen atoms.

In order to obtain insight into the relative stabilities of the two different polymorphs of $[Cu_2(H_2O)_{10}SiW_{12}O_{40}]\cdot 6H_2O$, we compared the Kohn-Sham energies from the DFT calculations on the monoclinic and triclinic phases. Details of the method are given in the experimental section. In both cases the geometry optimizations converged to give the lattice parameters and fractional coordinates that are in excellent agreement with our experimental results for both polymorphs, as listed in Table 1, supplementary information tables S3, S5 & S7. Furthermore, our calculations reveal that the monoclinic $P2_1/n$ phase, **2*c*,** is more stable than the triclinic *P*-1 phase, **2*t*,** with a ground-state energy difference of 0.309 eV per formula unit (while this may seem a large number for two polymorphs, note that we are dealing with a very large formula unit). The higher stability of the monoclinic phase is most likely related to the hydrogen bonding since the crystallographic densities of the two phases are very similar. While it is difficult to extract the hydrogen bond energies from the DFT calculations, the average $H\cdots O$ bond distance in the monoclinic phase is 1 % smaller than in the triclinic phase implying stronger bonds and greater stability. The higher stability of the monoclinic **2c** phase is in qualitative agreement with the PXRD analysis, which proves that bulk polycrystalline sample is dominated by this phase.

It is noteworthy that Cu^{II} alone behaves as a charge balancing cation to form $[Cu_{1.5}(H_2O)_{7.5}PW_{12}O_{40}]\cdot 4.75H_2O$ and $[Cu_2(H_2O)_{10}SiW_{12}O_{40}]\cdot 6H_2O$ crystals without the aid of any alkali metal as a counter cation. We also note that slow reaction kinetics at room temperature, coupled with the use of an ethanol:H_2O mixture as a solvent, results in the formation of high quality Cu^{II}-decorated POM crystals. By contrast, the use of higher reaction temperatures and aqueous conditions in the previously reported work by Méndez et. al.[35] did not yield highly crystalline products. In order to confirm the importance of the solvent conditions, we performed additional reactions in pure H_2O & pure ethanol and found that no crystals formed, even after several months.

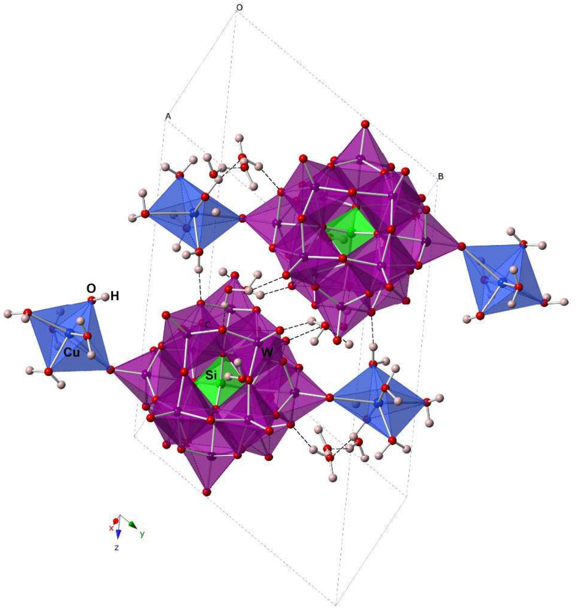

Figure 3: Compound 2*t*: Image showing the triclinic $[Cu_2(H_2O)_{10}SiW_{12}O_{40}]\cdot 6H_2O$ structure after the addition of H atoms followed by DFT optimization/MD simulations. The dotted lines indicate hydrogen-bonds between oxygen and hydrogen atoms.

Experimental Section

All chemicals were purchased from Sigma Aldrich and used without further purification. Single-crystal X-ray diffraction was performed on an Oxford Diffraction Gemini E Ultra diffractometer using Mo K_α radiation ($\lambda = 0.71073$ Å) operating at 50 kV and 40 mA. Full data sets were collected at approx. 125 K for all compounds. Data collection and reduction were performed using CrysAlisPro (version 1.171.37.35) from Agilent Technologies. An analytical numeric absorption correction using a multifaceted crystal model together with an empirical absorption correction using spherical harmonics was applied as implemented in CrysAlisPro (version 1.171.37.35). All the structures were solved using direct methods and subsequently refined by the full matrix least-squares procedure on F^2 using SHELXS and SHELXL within the OLEX2 interface.[42,43] Most atoms have been refined with anisotropic displacement parameters. However, partially occupied water molecules of compound **1** were refined isotropically. Hydrogen atoms could not be located in the difference map due to poor scattering contrast, and have hence not been included in the experimental structures. Thermogravimetric analysis was performed using TA instruments Q50 analyzer. PXRD measurements were performed using Bruker D8 Advance diffractometer in Bragg-Brentano (theta-theta) geometry. Infrared spectroscropy measurements were performed using a Bruker Tensor 27 FTIR. Igor Pro (version 6.37) by WaveMetrics was used to plot all graphs and CrystalMaker (version 9.0.4) was used to make all the images except for Figure 1 for which, Diamond (version 4.0.4) was used.

^{31}P NMR spectroscopy: ^{31}P NMR spectra were recorded at 162 MHz using a Bruker Biospin GmbH 400 spectrometer. Phosphoric acid (85 %) was used as an external reference. The solutions were prepared in 10 ml of D_2O or acetonitrile-d_6 (0.1 g of $[Cu_{1.5}(H_2O)_{7.5}PW_{12}O_{40}]\cdot 4.75H_2O$) respectively.

Synthesis of Compound I, Compound 2*c* & 2*t*

2.8 g of $Cu(NO_3)_2.3H_2O$ was dissolved in 20 ml of 50 vol% ethanol:H_2O. To this 1.5 g of $H_3PW_{12}O_{40}\cdot 12H_2O$ was added and the solution was stirred until all the acid dissolved. The solution was then left under static conditions at room temperature for four weeks. Light blue crystals of $[Cu_{1.5}(H_2O)_{7.5}PW_{12}O_{40}]\cdot 4.75H_2O$ emerged from the solution. A similar procedure was adopted for the synthesis of $[Cu_2(H_2O)_{10}SiW_{12}O_{40}]\cdot 6H_2O$; however, the starting acid used was $H_4SiW_{12}O_{40}\cdot 16H_2O$. %Yield: 44.36 of $[Cu_{1.5}(H_2O)_{7.5}PW_{12}O_{40}]\cdot 4.75H_2O$ and 42.69 of $[Cu_2(H_2O)_{10}SiW_{12}O_{40}]\cdot 6H_2O$ were obtained. The crystals were then used for further characterization both under dry and wet conditions. Similar syntheses in pure water and pure ethanol did not result in any crystal formation. The syntheses of both $[Cu_{1.5}(H_2O)_{7.5}PW_{12}O_{40}]\cdot 4.75H_2O$ and $[Cu_2(H_2O)_{10}SiW_{12}O_{40}]\cdot 6H_2O$ in 50 vol% ethanol:H_2O were performed at a higher temperature (40 °C) for 24 h. This resulted in the formation of powders of the respective compounds but no single crystals were obtained. The solubility of the compounds was checked in various solvents such ethanol, water, acetonitrile, methanol and cyclohexane. Compound **1** was soluble in all the solvents and compound **2** was soluble in all solvents except for acetonitrile and water.

Computational Details

In the crystallographic study, the positions of all atoms of the $[Cu_2(H_2O)_{10}SiW_{12}O_{40}]\cdot 6H_2O$ polymorphs are well defined except the hydrogen atoms. Therefore, in order to generate starting positions for the hydrogen atoms for the DFT calculations, we performed short NVE molecular dynamics (MD) simulations using the LAMMPS package.[44] The TIP4P model was used for the water molecules[45] and the ReaxFF force field for the other atoms.[46] The effect of van der Waals interactions were included during structural optimization. The simulations were performed at 298 K for 5 ps and then quenched to 0 K. The resulting forces on the ions were less than 10^{-6} kcal/mol/Å and the energy was converged to within10^{-4} kcal/mol.

Having obtained a reasonable initial structure from the MD simulations, first-principles density-functional theory (DFT) calculations were performed on the basis of the generalized gradient approximation (GGA) and the GGA + U method[47] implemented with the projector augmented wave (PAW)[48] pseudopotentials using the Vienna *ab-initio* Simulation Package (VASP).[49,50] The effects of van der Waals interactions were included during structural and electronic relaxation.[51] All of the DFT calculations were performed using (i) the plane-wave cut-off energy of 500 eV and (ii) the tetrahedron method with the Blöchl corrections for the Brillouin zone integrations.[52] A value of 5 eV was chosen for the Hubbard U_{eff} on Cu 3*d* states. We explicitly treated 11 valence electrons for Cu ($3d^{10}4s^1$), 4 for Si ($3s^23p^2$), 6 for W ($5d^46s^2$), 6 for O ($2s^22p^4$), and 1 for H ($1s^1$). For the monoclinic $P2_1/n$ cell, a $5\times3\times5$ Monkhorst–Pack *k*-point mesh[53] centered at Γ was used while a $5\times5\times5$ Monkhorst-Pack *k*-point grid was adopted for the triclinic P_1 cell. All structural relaxations were performed with a Gaussian broadening of 0.05 eV.[54] The ions were relaxed until the forces on them were less than 0.02 eV · A^{-1}.

Conclusions

Our study has shown that single crystals of $[Cu_{1.5}(H_2O)_{7.5}PW_{12}O_{40}]\cdot 4.75H_2O$ and $[Cu_2(H_2O)_{10}SiW_{12}O_{40}]\cdot 6H_2O$ can be obtained by adopting very slow reaction kinetics while tuning the solvent conditions. The behaviour of these crystals in different solvents is currently under investigation for possible application in photocatalysis. It is found that while the copper sites in the phosphotungstate structure are disordered, the $[Cu_2(H_2O)_{10}SiW_{12}O_{40}]\cdot 6H_2O$ forms two polymorphs containing *cis*- and *trans*-decorated Keggin isomers, which has not been observed previously for salts of polyoxoanions. DFT calculations reveal that the water modules can stabilize the crystal structures *via* different types of hydrogen-bonding. They also reveal that the *cis* polymorph is more stable than the *trans* form.

Acknowledgements

SB thanks the European Commission (FP7) for a Marie Curie postdoctoral fellowship (IEF). SH acknowledges the Alexander von Humboldt Foundation for a Feodor Lynen Return Fellowship. The DFT calculations were performed at the UK National Supercomputing Service, ARCHER, for which access was obtained via the UKCP consortium and funded by EPSRC under Grant No. EP/K014560/1.

References

1 M. T. Pope, *Polyoxometalate Molecular Science*, 2003, 3–31.
2 I. Kozhevnikov, *Chemical Reviews*, 1998, 171–198.
3 L. Ouahab, *Chem. Mater.*, 1997, **9**, 1909–1926.
4 M. Misono and M. Nojiri, *Appl. Catal.*, 1990, **64**, 1.
5 M. T. Pope and A. Müller, *Angew. Chem. Int. Ed. Engl.*, 1991, **39**, 34–48.
6 T. Yamase, *Chemical Reviews*, 1998, 307–325.
7 O. A. Kholdeeva, N. V. Maksimchuk and G. M. Maksimov, *Catalysis today*, 2010, **157**, 107–113.
8 N. V. Maksimchuk, K. A. Kovalenko, S. S. Arzumanov, Y. A. Chesalov, M. S. Melgunov, A. G. Stepanov, V. P. Fedin and O. A. Kholdeeva, *Inorg. Chem.*, 2010, **49**, 2920–2930.
9 U. Kortz, N. K. Al-Kassem, M. G. Savelieff, N. A. Al Kadi and M. Sadakane, *Inorg. Chem.*, 2001, **40**, 4742–4749.
10 D.-L. Long, R. Tsunashima and L. Cronin, *Angew. Chem. Int. Ed.*, 2010, **49**, 1736–1758.
11 U. Kortz, A. Müller, J. van Slageren, J. Schnack, N. S. Dalal and M. Dressel, *Coord. Chem. Rev*, 2009, 2315–2327.
12 C. L. Hill, *Chemical Reviews*, 1998, **98**, 1–2.
13 R. I. Maksimovskaya, *Journal of Structural Chemistry*, 2006, **47**, 952–978.
14 F. Goubin, L. Guénée, P. Deniard, H. J. Koo, M. H. Whangbo, Y. Montardi and S. Jobic, *J. Solid State Chem.*, 2004, **177**, 4528–4534.
15 X. López, J. M. Maestre, C. Bo and J. M. Poblet, *J. Am. Chem. Soc.*, 2001, **123**, 9571–9576.
16 L. Lisnard, A. Dolbecq, P. Mialane, J. Marrot, E. Codjovi and F. Sécheresse, *Dalton Transactions*, 2005, **24**, 3913–3920.
17 V. S. Bryantsev, M. S. Diallo, A. C. T. van Duin and W. A. Goddard III, *The Journal of Physical Chemistry A*, 2008, **112**, 9104–9112.
18 Y. P. Jeannin, *Chemical Reviews*, 1998, 51–76.
19 P. Gouzerh and A. Proust, *Chemical Reviews*, 1998, **98**, 77–111.
20 Y. Izumi, K. Urabe and M. Onaka, *Kodansha/VCH: Tokyo,*, 1992, 99.
21 M. A. Schwegler and H. van Bekkum, *Bull. Soc. Chim. Belg.*, 1990, **99**, 113–120.
22 C. L. Hill and C. M. Prosser-McCartha, *Coord. Chem. Rev*, 1995, **143**, 407–455.
23 J. H. Grate, D. R. Hamm and S. Mahajan, *Molecular Engineering*, 1993, **3**, 205–229.
24 W. H. Knoth, P. J. Domaille and R. L. Harlow, *Inorg. Chem.*, 1986, 1577–1584.
25 L. R. Pizzio, C. V. Caceres and M. N. Blanco, *Appl. Catal. A.*, 1998, **167**, 283–294.
26 J. S. Yadav, B. V. S. Reddy, K. V. Purnima, K. Nagaiah and N. Lingaiah, *J. Mol. Catal. A: Chem.*, 2008, **285**, 36–40.
27 K. V. Purnima, D. Sreenu, N. Bhasker, K. Nagaiah, N. Lingaiah, B. V. Subba Reddy and J. S. Yadav, *Chinese Journal of Chemistry*, 2013, **31**, 534–538.
28 S. S. Mal and U. Kortz, *Angew. Chem. Int. Ed.*, 2005, **44**, 3777–3780.
29 P. Mialane, A. Dolbecq, J. Marrot, E. Rivière and F. Sécheresse, *Chemistry - A European Journal*, 2005, **11**, 1771–1778.
30 H. An, E. Wang, Y. Li, Z. Zhang and L. Xu, *Inorganic Chemistry Communications*, 2007, **10**, 299–302.
31 J. M. Clemente-Juan and E. Coronado, *Coordination Chemistry Reviews*, 1999, **193-195**, 361–394.
32 K. Brown, P. E. Car, A. Vega, D. Venegas-Yazigi, V. Paredes-García, M. G. F. Vaz, R. A. Allao, J.-Y. Pivan, E. Le Fur and E. Spodine, *Inorganica Chimica Acta*, 2011, **367**, 21–28.
33 T. T. Ali, S. A. Al-Thabaiti, A. O. Alyoubi and M. Mokhtar, *Journal of Alloys and Compounds*, 2010, **496**, 553–559.
34 S. Aravind and N. Reddy, *Helvetica Chimica Acta*, 2015, **98**, 557–560.
35 L. Méndez, R. Torviso, L. Pizzio and M. Blanco, *Catal. Today*, 2011, **173**, 32–37.
36 S. R. Bajpe, C. E. A. Kirschhock, A. Aerts, E. Breynaert, G. Absillis, T. N. Parac-Vogt, L. Giebeler and J. A. Martens, *Chemistry - A European Journal*, 2010, **16**, 3926–3932.
37 S. R. Bajpe, E. Breynaert, D. Mustafa, M. Jobbágy, A. Maes, J. A. Martens and C. E. A. Kirschhock, *Journal of Materials Chemistry*, 2011, **21**, 9768.
38 S. R. Bajpe, E. Breynaert, A. Martin-Calvo, D. Mustafa, S. Calero, C. E. A. Kirschhock and J. A. Martens, *ChemPlusChem*, 2013, **78**, 402–406.
39 D. Mustafa, I. G. N. Silva, S. R. Bajpe, J. A. Martens, C. E. A. Kirschhock, E. Breynaert and H. F. Brito, *Dalton Transactions*, 2014, **43**, 13480–13484.
40 N. Janssens, L. H. Wee, S. Bajpe and E. Breynaert, *Chemical Science*, 2012, **3**, 1847–1850.
41 J. Canny, A. Teze, R. Thouvenot and G. Hervé, *Inorg. Chem.*, 1986, **25**, 2114–2119.
42 O. V. Dolomanov, L. J. Bourhis, R. J. Gildea, J. A. K. Howard and H. Puschmann, *J Appl Cryst*, 2009, **42**, 339–341.
43 G. M. Sheldrick, *Acta Cryst A*, 2008, **64**, 112–122.
44 S. Plimpton, *J. Comput. Phys.*, 1995, **177**, 1–19.
45 W L Jorgensen et al, *J. Am. Chem. Soc.*, 1996, **118**, 11225–11236.
46 A. C. T. van Duin, S. Dasgupta, F. Lorant and W. A. Goddard, *The Journal of Physical Chemistry A*, 2001, **105**, 9396–9409.
47 S. L. Dudarev, S. Y. Savrasov, C. J. Humphreys and A. P. Sutton, *Phys. Rev. B*, 1998, **57**, 1505–1509.
48 P. E. Blöchl, *Phys. Rev. B*, 1994, **50**, 17953–17979.
49 G. Kresse and J. Hafner, *Phys. Rev. B*, 1993, **47**, 558–561.
50 G. Kresse and J. Furthmüller, *Phys. Rev. B*, 1996, **54**, 11169–11186.
51 J. Klime, D. R. Bowler and A. Michaelides, *Phys. Rev. B*, 2011, **83**, 1–13.
52 P. E. Blöchl, O. Jepsen and O. K. Andersen, *Phys. Rev. B*, 1994, **49**, 16223–16233.
53 J. D. Pack and H. J. Monkhorst, *Phys. Rev. B*, 1977, **16**, 1748–1749.
54 C. Elsässer, M. Fähnle, C. T. Chan and K. M. Ho, *Phys. Rev. B*, 1994, **49**, 13975–13978.